Development of novel pyrazolone derivatives as inhibitors of aldose reductase: An eco-friendly one-pot synthesis, experimental screening and *in silico* analysis

Aparna Kadam [a], Bhaskar Dawane [a], Manisha Pawar [a], Harshala Shegokar [b], Kapil Patil [b], Rohan Meshram [b], Rajesh Gacche [b,*]

[a] School of Chemical Sciences, Swami Ramanand Teerth Marathwada University, Nanded (MS), India
[b] School of Life Sciences, Swami Ramanand Teerth Marathwada University, Nanded (MS), India

ABSTRACT

Aldose reductase is the key enzyme of polypol pathway leading to accumulation of sorbitol. Sorbitol does not diffuse across the cell membranes easily and therefore accumulates within the cell, causing osmotic damage which leads to retinopathy (cataractogenesis), neuropathy and other diabetic complications. Currently, aldose reductase inhibitors like epalrestat, ranirestat and fidarestat are used for the amelioration of diabetic complications. However, such drugs are effective in patients having good glycemic control and less severe diabetic complications. In present study we have designed novel pyrazolone derivative and performed eco-friendly synthesis approach and tested the synthesized compounds as potential inhibitors of aldose reductase activity. Additional *in silico* analysis in current study indicates presence of highly conserved chemical environment in active site of goat lens aldose reductase. The reported data is expected to be useful for developing novel pyrazolone derivatives as lead compounds in the management of diabetic complications.

© 2014 Elsevier Inc. All rights reserved.

1. Introduction

In recent past, diabetes was believed to be associated with overindulgent life-style and thus was thought as major health concern in industrialized countries. Recent reports have revealed that this disease has now engulfed entire globe, specifically India is suspected to have around 15 million people suffering from this disease [1,2]. The pathogenesis of the diabetic complications entails multifaceted aspects and hence many mechanisms are proposed for its origin; however, one of the major proposed theories for development of the diabetic complications involves the polyol pathway [3]. According to a study involving polymorphic markers of the human aldose reductase (AR) gene, a very strong association is observed between expression of AR gene and susceptibility to develop diabetic complications. These observations point towards the key role of AR in development of diabetes in human [4–6]. Despite of several recent reports describing *in vitro* and experimental animal models involving AR inhibition and significant protection against diabetic complications [7–9], a successful drug is still yet

to be developed. Thus, research on AR inhibition currently dominates the area of anti-diabetic therapeutics regimen.

Compounds containing pyrazolone as parent scaffold are known to have wide varieties of therapeutic applications. These compounds are used as starting material for the synthesis of various biologically active compounds [10]. Pyrazolone derivatives are an important class of heterocyclic compounds that occur in many drugs and synthetic products [11,12], and thus exhibit a wide spectrum of biological properties including anti-microbial, anti-bacterial, anti-fungal, anti-oxidant, anti-gout activities [13]. Pyrazole and its synthetic analogs have been reported to possess industrial, agricultural and some biological application. These compounds show remarkable anti-tubercular [14], analgesic [15], anti-inflammatory [16], anti-neoplastic [17] and anti-tumor activity [18]. A very recent research describing anti-diabetic activity of pyrazolone containing compounds [19], promoted us to investigate the possibility of AR inhibitory activity of pyrazolone derivatives.

In present work we describe efficient green synthesis of some novel pyrazolone derivatives followed by their *in vitro* screening and subsequent *in silico* analysis. The pyrazolone derivatives were synthesized by an eco-friendly approach using PEG-400 as a green solvent and bleaching earth clay (pH12.5) as a catalyst. Bleaching earth clay is easily available in India with very low cost and hence

are actively utilized on industrial scale for refining of vegetable oils (British Patent GB-1077557, 1970) fats, greases and used as catalyst in reactions (US Patent 4970295, 1990). The formed compounds were confirmed by spectroscopic methods.

2. Material and methods

Melting points were uncorrected and determined in an open capillary tube. IR spectras were recorded on FTIR Schimadzu spectrometer. ^{1}H NMR spectras were obtained in DMSO-d6 on avance 300 MHz spectrometer using TMS as an internal standard. The mass spectra were documented on EI-Shimadzu-GC–MS spectrometer.

2.1. Synthesis of pyrazolone derivatives

2.1.1. General procedure for the synthesis of 3-amino-4-(4^I-substituted benzylidene)-1H-pyrazol-5(4H)-one derivatives

An equimolar mixture of substituted benzaldehyde/heteroaldehyde (1 mmol), ethylcyanoacetate (1 mmol), was heated in PEG-400(20 ml) at 40–50 °C for 4–5 h. After completion of reaction (monitored by TLC), add 5–10 ml Hydrazine hydrate 99% with continuous heating. After the completion of reaction, the crude mixture was worked up in ice-cold water (100 ml). The product was separated by using filtration. The filtrate was evaporated to remove water and PEG leaving behind and obtained corresponding products (1a-e). The purity of the synthesized compound was checked by TLC on microscopic slide with silica gel layer. The structures of compounds were assigned on the basis of spectral data such as IR, NMR and MASS.

2.1.2. General procedure for the synthesis of 3-amino-4-(4I-substitued benzylidene)-4,5-dihydro-5-oxopyrazole-1-carbothioamide derivatives

An equimolar mixture of substituted benzaldehyde/heteroaldehyde (1 mmol), ethylcyanoacetate (1 mmol) and thiosemicarbazide (1 mmol) was heated in PEG-400 (20 ml) at 50–60 °C for 4–5 h. After completion of reaction (monitored by TLC), the crude mixture was worked up in ice-cold water (100 ml). The product was separated by filtration. The filtrate was evaporated to remove water and PEG leaving behind and obtained corresponding products (2a-e). The purity of the synthesized compounds was checked by TLC on microscopic slide with silica gel layer. The structures of compounds were assigned on the basis of spectral data such as IR, NMR and MASS. Both the above schemes are represented in Fig. 1.

The resulting compounds via the schemes with both series (1a-e) and (2a-e) described above are represented in supplementary Fig. 1.

2.1.3. Spectroscopic data of selected compounds

3-Amino-4-(4I-chloro benzylidene)-1H-pyrazol-5(4H)-one (1a). **IR (KBr):**3363(—NH)cm^{-1}, 3063(—CH=)cm^{-1}, 3009(Ar—H)cm^{-1}, 1705(>C=O)cm^{-1}, 1543(C=N)cm^{-1}, 1234(—N—N—C of pyrazole)cm^{-1}, 600–800(C—Cl)cm^{-1}, **^{1}H NMR** (DMSO-d6): δ4.7 (s, 2H, NH$_2$), δ6.7(s, 1H, =CH), δ7.6(d, 2H, Ar—H), δ7.9(d, 2H, Ar—H), δ8.7(s, 1H, —NH), **EIMS(m/z):** 221.47(M$^+$).

3-Amino-4-(4I-fluoro benzylidene)-1H-pyrazol-5(4H)-one (1b). **IR (KBr):**3420(—NH)cm^{-1}, 3090(—CH=)cm^{-1}, 2928(Ar—H)cm^{-1}, 1629(>C=O)cm^{-1}, 1600(C=N)cm^{-1}, 1225 (—N—N—C of pyrazole)cm^{-1}. **^{1}H NMR** (DMSO-d6): δ4.8(s, 2H, NH$_2$), δ6.8(s, 1H, =CH), δ7.1(d, 2H, Ar—H), δ7.8(d, 2H, Ar—H), δ8.6(s, 1H, NH), **EIMS (m/z):** 205.35(M$^+$).

3-Amino-4-[3-(4I-methoxyphenyl)-1-phenyl-1H-pyrazol-5-yl)methylene]-1H-pyrazol-5(4H)-one (1d). **IR (KBr):** 3440 (—NH)cm^{-1}, 3071(—CH=)cm^{-1}, 2921(Ar—H)cm^{-1}, 1670(>C=O)cm^{-1}, 1593(C=N)cm^{-1}, 1213(—N—N—C of pyrazole)cm^{-1}. **^{1}H NMR (DMSO-d$_6$):** δ3.9(s, 3H, —OCH$_3$), δ4.5(s, 2H, NH$_2$), δ6.2(s, 1H, =CH), δ7.2–8.0(m, 10H, Ar—H and —CH of pyrazole), δ8.6(s, 1H, NH).

3-Amino-4-(4I-fluoro benzylidene)-4,5-dihydro-5-oxopyrazole-1-carbothioamide (2b). **IR (KBr):** 3302(—NH)cm^{-1}, 3011(—CH=)cm^{-1}, 2933(Ar—H)cm^{-1}, 1654(>C=O)cm^{-1}, 1609(C=N)cm^{-1}, 1230(—N—N—C of pyrazole)cm^{-1}, 1184(C=S)cm^{-1}. **^{1}H NMR (DMSO-d$_6$):** δ4.2(s, 2H, —NH$_2$), δ6.5(s, 1H, —CH=), δ7.0–7.9(m, 4H, Ar—H), δ9.8(s, 2H, $\overset{}{\underset{H_2N}{\diagup}}$=S). **13C NMR (CDCl$_3$):** δ189.42, δ166.42, δ163.08, δ160.96, δ130.71, δ130.60, δ130.50, δ130.46, δ129.93, δ116.29, δ116.00.
    EIMS (M/z): 263(M$^+$).

2.2. Biological activity

AR activity was checked by goat lens aldose reductase inhibition assay. The AR inhibitory activity was measured according to the method described earlier by Suryanarayana et al. [20]. The reaction cocktail contained 1 ml of 1 M potassium phosphate buffer (pH 6.2), 0.4 mM lithium sulfate and 5 μM 2-mercaptoethanol, 10 μM DL-glyceraldehydes, 0.1 μM NADPH, and crude enzyme. The reaction mixture was incubated at 37 °C for 10 min. The enzymatic
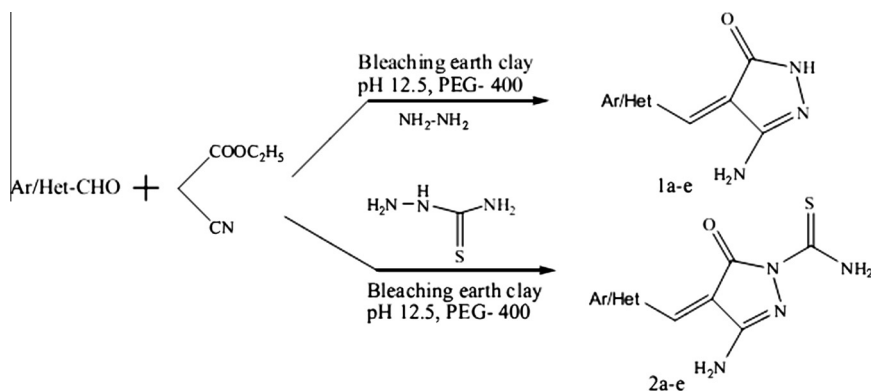

Fig. 1. Scheme for preparation of derivatives from 1a–e and 2a–e.

reaction was initiated by addition of NADPH and activity was measured by recording the decrease in absorbance at 340 nm. Various concentrations of selected compounds were added to assay mixture and appropriate blanks were prepared for correction. AR activity in the absence of inhibitor was considered as 100% for the determination of IC50 values, the concentration of individual compounds required to achieve 50% AR inhibition were calculated. Quercetin (IC50, 3.12 μM/ml) was used as a standard AR inhibitor.

2.3. Docking investigation

2.3.1. Ligand preparation
2D structures of all compounds were drawn in ChemDraw 8.0 (CambridgeSoft, Cambridge, MA, USA) and their SMILES were obtained. The 3D conformers of these compounds were then generated in SDF format using FROG2 server [21]. Autodock 4.0 [22,23] implemented in python prescription 0.8 (PyRx) was used in docking analysis. The ligand molecules in sdf format were imported in PyRx environment via OpenBabel utility and were subject to energy minimization using UFF forcefield [24–26], Conjugate gradient optimization algorithms was applied for over 200 steps while molecules were updated for every 1 step.

2.3.2. Receptor preparation
Structural model of AR in complex with zopolrestat with PDB ID 2DUX was downloaded from protein data bank [27]. This monomeric structural model of AR was co-crystallized with solvent molecules, inhibitor zopolrestat along with its essential prosthetic group nicotinamide adenine dinucleotide phosphate (NADP). Receptor molecule was prepared in traditional pdbqt format after assigning charges to the receptor coordinate file by using 'Make macromolecule' command from Autodock menu of PyRx.

2.3.3. Testing validity of AutoDock 4.2 and virtual screening
The validity of a docking system can be checked by docking the experimentally verified pose back into the receptor. This procedure follows the rationale that a good docking engine should replicate the experimental binding modes of the ligand. After docking, root mean square deviation (RMSD) value of the predicted pose to experimentally verified pose is calculated. RMSD value indicates the measure of spatial similarity between two structures. If the RMSD value is found to be less than certain value (typically <2.00 angstrom), the prediction of binding mode is considered as successful. Auto-grid program was utilized to obtain grid file. The affinity grid of 50 × 50 × 50 points was set using spacing of 0.375 angstrom in order to encompass entire active site. The lamarckian genetic algorithm was used for the conformational search. Each lamarckian job was set to have 10 runs. The initial population was restricted to 150 structures; while the maximum number of energy evaluation and generation were set to 27,000. Single top individual was allowed to survive to next generation, rate of gene mutation was set to 0.02 and rate of crossover was set to 0.8; the rest of parameters were set to default values. The final structures were clustered and according to native autodock scoring function. RMSD value of 0.43 angstrom was obtained from the re-docking experiment of zopolrestat. This value indicates that predicted binding mode is nearly identical to the X-ray crystallography conformer (supplementary Fig. 2). Same settings were used to dock selected pyrazolone derivatives. The top ranked conformations of each ligand were selected.

2.3.4. Post virtual screening analysis (paired potential analysis)
Further analysis of docked conformers were carried out using on-line program DSX-ONLINE v0.88, knowledge-based DSX pair potentials that are based on the Drug Score potential [28]. Results obtained from docking and those from DSX server were visualized

in PyMol. Two dimensional schematic representation of inhibitor with residues from active site were generated using Ligplot+ [29,30].

3. Results and discussion

3.1. Chemical synthesis

We have realized that processes for synthesizing chemical products are highly inefficient and it has been estimated that for every kilogram of fine chemical and pharmaceutical products produced, 5–100 times that amount of chemical waste is generated [31]. The prime component of waste in the majority chemical productions is related with use of solvent, hence as part of green chemistry efforts, various cleaner solvents have been proposed as safer substitution [32]. It has now been proved that solvent PEG-400 is not only an environmentally benign reaction solvent but also non-toxic, inexpensive, water soluble (which facilitates its removal from the reaction product) and is highly reusable [33,34]. Hence we have utilized this green solvent in conjugation with bleaching earth clay that is used as a catalyst which is also fully recyclable and can be collected from the reaction by simple filtration and thus are essential requirements for the principles of green chemistry. Considering an ever increase concern towards the development of new environmental friendly synthesis procedures for the production of biologically active compounds, here we reported an efficient method for the synthesis of 3-amino-4-(4ᴵ-substituted benzylidene)-1H-pyrazol-5(4H)-one and 3-amino-4-(4ᴵ-substitued benzylidene)-4,5-dihydro-5-oxopyrazole-1-carbothioamide by simultaneous one pot condensation of substituted aldehyde/heteroaldehyde, ethylcyano acetate, hydrazine hydrate (99%) and thiosemicarbazide by using PEG-400 and bleaching earth clay(pH12.5).

The reaction time, yield and melting point of pyrazolone derivatives are described in Table 1 and Table 2. The reactions proceed rapidly and completed within 4–5 h. The newly synthesized compounds 1a-e and 2a-e were established on the basis of spectroscopic data. IR spectra of pyrazolone and pyrazole-1-carbothioamide derivatives showed characteristic peak in between 3400

Table 1
Table showing data for synthesis of 3-amino-4-(4ᴵ-substituted benzylidene)-1H-pyrazol-5(4H)-one derivatives catalyzed by bleaching earth clay (pH 12.5) in PEG-400.
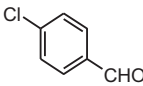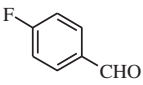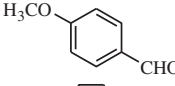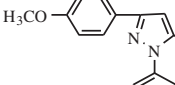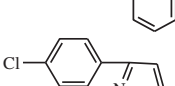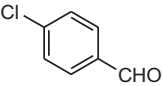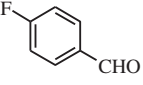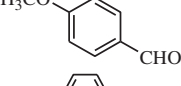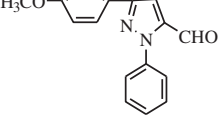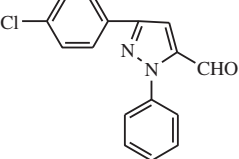
Compound code	(Aromatic/heterocyclic aldehydes)	Time (h)
1a		3.0
1b		4.0
1c		3.5
1d		3.0
1e		4.5

Table 2
Table showing data for synthesis of 3-amino-4-(4^I-substitued benzylidene)-4,5-dihydro-5-oxopyrazole-1-carbothioamide derivatives catalyzed by bleaching earth clay (pH 12.5) in PEG-400.

Compound code	(Aromatic/heterocyclic aldehydes)	Time (h)
2a		4.0
2b		4.5
2c		3.5
2d		4.5
2e		4.0

and 3500 cm^{-1} due to —NH$_2$. The peak at 1650–1690 cm^{-1} is due to >C═O stretch vibrations. The peak was observed at 1200–1235 cm^{-1} due to (—N—N—C of pyrazole ring), while the peak was observed at 1270–1190 cm^{-1} due to C═S stretching. Beside these bands 680–800 cm^{-1} due to C—Cl stretching whenever present in the compound. ^{1}H NMR spectra of compounds were studied in CDCl$_3$ and DMSO showed characteristic peak at δ 3.9 ppm of —OCH$_3$, peak at δ6.6 ppm of —CH═CH, δ7–8 ppm of Aromatic protons, the characteristic peak was observed at δ8.6–9.0 ppm of –NH of pyrazole ring. The peak was observed at δ4.6 ppm of —NH$_2$. The peak was observed at δ9.8 ppm of ⟨image⟩. The mass spectra of these compounds were showed molecular ion peak corresponding to their molecular formula.

3.2. Biological evaluation

All the compounds produced by both the schemes were evaluated for their AR inhibitory activity in terms of IC50 values. The results of *in vitro* AR activity are presented in Table 3. Out of 5 compounds produced in scheme 1, first three compounds, 1a, 1b and 1c showed a little inhibitory activity (IC50 values 16.70 μM, 18.80 μM and 17.60 μM respectively). This might have occurred due to direct attachment of hydrophobic chloro, fluoro and methoxy benzylidene moieties respectively to pyrazolone. Their lower potency towards AR inhibition is further explained using paired potential analysis in upcoming sections.

But when this substituted benzylidene group was replaced by 3-(4^I-methoxyphenyl)-1-phenyl-1H-pyrazole group yielded compound 1d. These substitutions resulted in its sudden improved performance (two fold improvement in IC50) as shown in Table 3. In compound 1e, 3-(4^I-methoxyphenyl)-1-phenyl-1H-pyrazole was found to be placed at first position, this feature can be attributed to increased performance as compared to first three compounds (IC50 value 9.20 μM) indicating importance of proper positioning of pyrazole group in inhibition.

All compounds in second series contained carbothioamide group. First three compounds of second series (2a, 2b and 2c) still performed poor owing to direct connection of substituent chloro, fluoro and methoxy benzylidene fragments to pyrazolone, however it is to be noted that existence of carbothioamide group slightly improved inhibitory effect of these compounds (IC50 values 15.50 μM, 11.90 μM and 12.80 μM as compared to that of compound 1a, 1b and 1c described in previous paragraph) This observation is inductive of the fact that hydrophobic moieties like phenyl group directly attached with pyrazolone adversely affects inhibitory properties of AR. By virtue of replacement of phenyl substituents from previous compounds (1a, 1b, 1c, 2a, 2b and 2c) with 3-(4^I-methoxyphenyl)-1-phenyl-1H-pyrazole and 3-(4^I-chlorophenyl)-1-phenyl-1H-pyrazole (compound 1d, 2d and 1e, 2e); inhibitory potential significantly improved (for example IC50 of 8.10 μM in case of compound 2d). The best inhibition value among all the synthesized derivatives was observed in compound 2e (IC50 of 6.30 μM). This performance can be attributed to synergistic effect produced due to simultaneous presence of carbothioamide group and 3-(4^I-methoxyphenyl)-1-phenyl-1H-pyrazole and 3-(4^I-chlorophenyl)-1-phenyl-1H-pyrazole substituent at first position.

3.3. In silico evaluations

Binding cleft of target AR is approximately 10.84 angstrom deep containing NADP and Zopolrestat and possess huge volume of 3505.36 Å^3, since it is known to accommodate prosthetic group as well as substrate (or inhibitor) simultaneously, as observed from its binary complex structures [35]. This big cleft can be conceptually imagined to be formed by two main sub pockets. A hydrophobic pocket P1 is formed by residues 112-PTGF-115, 303-C, 309-YPFHE-313 and represented by cyan color. Pocket P1

Table 3
Aldose reductase inhibition results of selected pyrazolone and carbothioamide derivatives.

Compound code	Mol. formula	Mol. Wt.	M.P. (°C)	Yield%	Solubility	Aldose reductase activity IC$_{50}$ (μM)
1a	C$_{10}$H$_8$N$_3$OCl	221	178	83.33	DMSO	16.70
1b	C$_{10}$H$_8$N$_3$OF	205	185	82.41	DMSO	18.80
1c	C$_{11}$H$_{11}$N$_3$O$_2$	217	182	75.47	DMSO	17.60
1d	C$_{20}$H$_{17}$N$_5$O$_2$	359	240	81.78	DMSO	7.70[a]
1e	C$_{19}$H$_{14}$N$_5$OCl	363	248	69.45	DMSO	9.20[a]
2a	C$_{11}$H$_9$N$_4$OSCl	280	189	75.94	DMSO	12.50
2b	C$_{11}$H$_9$N$_4$OSF	264	184	85.10	DMSO	11.90
2c	C$_{12}$H$_{12}$N$_4$O$_2$S	264	210	82.25	DMSO	12.80
2d	C$_{21}$H$_{18}$N$_6$O$_2$	418	256	71.42	DMSO	8.10[a]
2e	C$_{20}$H$_{15}$N$_6$OSCl	422	248	74.62	DMSO	6.30[a]
Quercetin	–	–	–	–	–	3.12[b]

[a] Compounds showing promising IC$_{50}$ values.
[b] Standard compound.

is separated by residue 111-W via formation of separating wall (yellow color) that leads to pocket P2 which is lined by residues 110-H, 159-SN-160, 183-Q, 209-Y, 260-I and represented by orange color. Pocket P2 is in continuum with cavity that holds NADP (supplementary Fig. 3). Experimentally verified structure of AR in complex with zopolrestat illustrates vital interaction of trifluoromethyl moiety attached via benzothiazole scaffold of inhibitor with residues from pocket P1, while phthalazinone ring protrudes towards pocket P2 as seen in supplementary Fig. 3 [36,37].

It is reported that AR prefers highly hydrophobic compounds owing to its lipophilic active site [35,38]; the first three inhibitors of first series (1a, 1b and 1c) contained hydrophobic chloro, fluoro and methoxy benzylidene moieties attached to pyrazolone. Comparatively reduced inhibitory activity of these compounds can be effectively explained by its *in silico* docking and paired potential analysis.

Paired potential analysis of docked conformers enables to scrutinize the per-atom score contribution of inhibitor in active site of structural model in terms of 'good' and 'bad' potentials. These paired potential represent favorable and unfavorable interactions respectively. Favorably interacting atoms from inhibitor are depicted to be surrounded by blue spheres; while the sizes of the spheres correspond to the values of the contributing per-atom scores (Figs. 2 and 3). In simpler words, larger the sphere, more favorable is the interaction. If the inhibitor is not structurally competent with active site of enzyme, it makes unfavorable contacts with surrounding residues. Such unfavorable contacts are depicted as 'bad contacts' in paired potential analysis and are represented as red lines (refer Fig. 2 in case of compound 1a and 1b). Analyzing Fig. 2 it becomes evident that chloro and fluoro benzylidene moieties of compound 1a and 1b have shown to interact favorably in active site since these are hydrophobic moieties and preferred by hydrophobic enzyme active site [35,38], while amino pyrazolone containing region of same compounds makes numerous bad contacts (indicated by red lines) signifying unacceptable mode of binding. These unfavorable contacts thus results in lower binding

affinity as correlated in docking calculations (refer Table 4), binding energies −6.89 kcal/mol and −6.31 kcal/mol for 1a and 1b respectively). These facts might result in lower potency of compound 1a and 1b in AR inhibition. Similar results of binding affinity as well as paired potential analysis was obtained for compound 1c (figure not shown).

Literature survey indicate that carbothioamide moiety in many compounds is proved to be responsible for diverse biological activities including antibacterial, anti fungal [39,40], anti proliferative [41] as well as anti tumor [42,43], hence its presence in existing pyrazolone derivatives (compounds 2a, 2b and 2c) can be hypothesized to increase potency of AR inhibition activity. This assumption was verified to be convincing, since compound containing carbothioamide group in this study are found to increased inhibition to a little extent (IC 50 values improved to 12.50, 11.90 and 12.80 μM for compound 2a, 2b and 2c respectively). This improvement can be attributed to the fact that placement of this group seems to reorient the pyrazolone moiety, hence avoid the bad contacts and enable it to maintain favorable interaction in active site as observed from result of paired potential analysis. Fig. 2 also point out complete elimination of bad contacts and proper orientation of pyrazolone moiety to attain complimentary interactions with residues from active site. This fact is again supported by improvement in binding energies obtained from docking analysis for compounds 2a, 2b and 2c (−7.56, −7.06, −7.28 kcal/mol respectively).

Structural analysis of docking poses of previous compounds (1a, 1b, 1c, 2a, 2b and 2c) revealed the fact that due to small size of all the above compounds, they may not occupy both the binding pockets. Better results are observed for compounds that are absolutely complemented to active site area (i.e. compounds 1d, 1e, 2d, 2e). These compounds possess optimally placed hydrophobic moieties attached to parent pyrazolone via methylene bridges. These structural features can be suspected for striking improvement in observed AR inhibition. These structural peculiarities might result in improvement by approximately 3 folds (IC 50 6.30 μM in case of inhibitor 2e as compared to initial 18.80 μM for compound 1b).
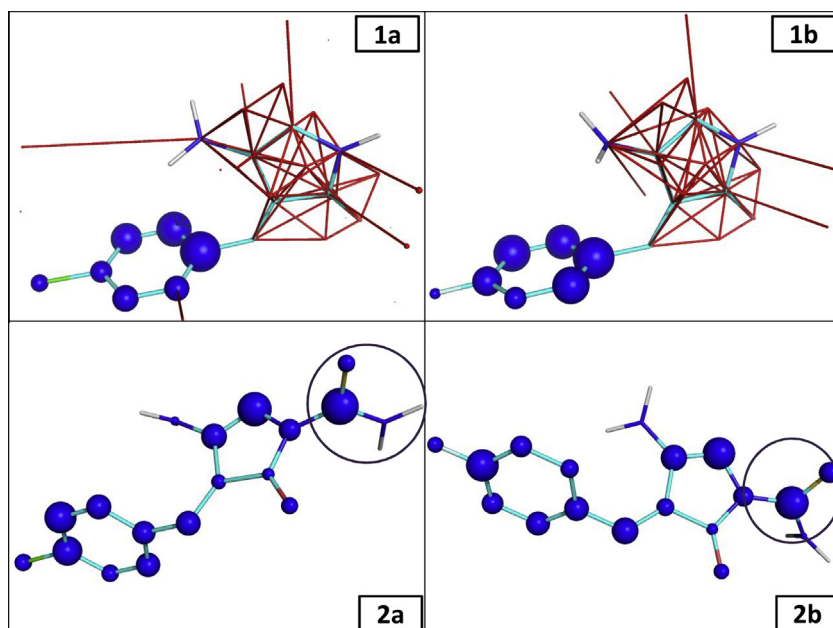

Fig. 2. Figure showing paired potential analysis results for compound 1a, 1b, 2a and 2b (CPK colored sticks). Atoms surrounded by blue sphere indicate paired potential per-atom score while red lines surrounding amino pyrazole moiety (compound 1a and 1b) represent bad contacts with residues in active site (residues in active site are not shown here for sake of clarity). For compound 2a and 2b, note improvement in per atom score of amino pyrazole moiety resulted due to introduction of carbothioamide group (highlighted by circle).
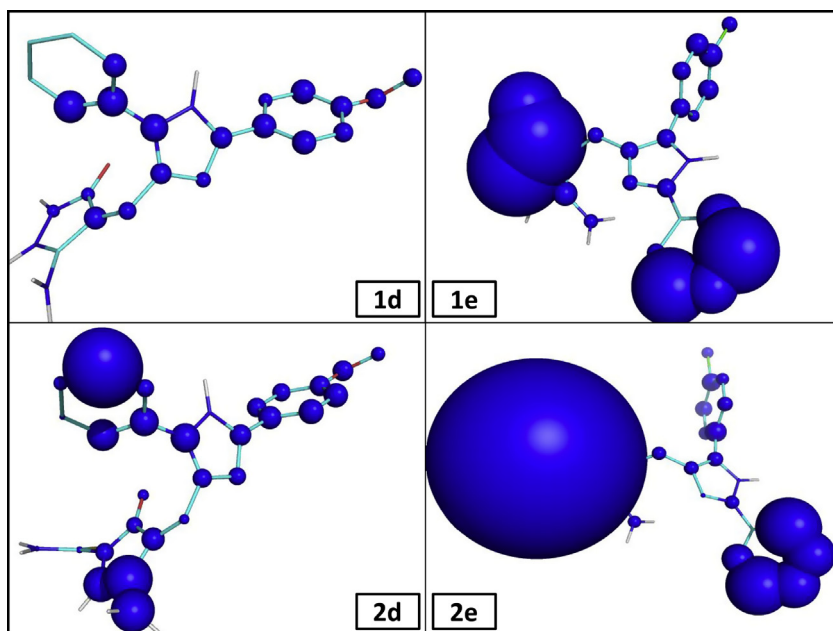
Fig. 3. Figure showing paired potential analysis results for compound 1d, 1e, 2d and 2e (CPK colored sticks). Atoms surrounded by blue sphere indicate paired potential per-atom score. Note significant improvement in per atom score depicted as large blue spheres.

Table 4
Molecular docking results of selected pyrazolone and carbothioamide derivatives.

Name of ligand	Binding energy
Zopolrestat	−10.59[a]
1a	−6.89
1b	−6.31
1c	−6.56
1d	−8.64[b]
1e	−9.32[b]
2a	−7.56
2b	−7.06
2c	−7.28
2d	−9.35[b]
2e	−10.58[b]

[a] Experimentally crystallized inhibitor, used as reference structure to validate accuracy of autodock algorithm.
[b] Compounds showing best binding affinity towards aldose reductase.

These structural features seems to bring about exact complementary of compounds to active site resulting in proper placement of hydrophobic moieties in respective binding pockets. These facts are evident from structural analysis of docking results as well as from paired potential analysis (Fig. 3).

3.4. Structural analysis of docking results

3.4.1. Structural analysis of docking results for compound 1d

Methoxy benzylidene moiety of compound 1d is found to be stack on heterocyclic aromatic side chain of Trp 111. Such stacking interaction with Trp 111 is found to be one of basic force stabilizing experimentally observed inhibitors [36]. Moreover, N1 atom of central pyrazole ring seems to make ionic contact with NE1 atom of Trp 111 (Fig. 4a). More than half of the van der Waals contacts between inhibitor and residues of active site are formed between carbon atoms, demonstrating that enzyme–inhibitor interaction are highly hydrophobic in nature (Fig. 4a and b).

3.4.2. Structural analysis of docking results for compound 1e

Amino-pyrazole moiety of compound 1e is found to be involved in polar contacts with side chains of residues in active site. N3 atom of amino pyrazole appears to form hydrogen bond with O atom of Tyr 48 side chain (Fig. 4c). In a study involving inhibition of AR by citrate and cacodylate as inhibitors revealed critical role of polar interaction involving Tyr 48 as observed in present study [44]. SG sulfur atom of thiol group from Cys 298 forms a salt bridge with keto oxygen of amino pyrazole portion of compound1e (Fig. 4c). Inhibitor's interaction observed in present study with Cys 298 is experimentally verified to be essential for inhibition of AR [45,46]. Chloro-phenyl part of inhibitor occupies P1 hydrophobic pocket lined by residues Cys 303, Phe 122, Leu 300, and Trp 79; while P2 pocket is occupied by amino-pyrazole moiety imparting total complementary with that of active site (Fig. 4d).

3.4.3. Structural analysis of docking results for compound 2d

Terminal anisole group of compound 2d seems to occupy P1 pocket, simultaneously making an ionic contact via its O2 oxygen atom with OG1 atom of Thr 113 side chain (Fig. 5a and b). Such ionic contacts via Thr 113 are experimentally verified to be critical in inhibition of AR for inhibitors like fidarestat (SNK-860) and minalrestat (WAY-509) [47]. Benzyl group of ligand completely occupies P2 pocket. N6 atom of carbothioamide component of compound 2d seems to be hydrogen bonded with backbone oxygen of Val 47 thus stabilizing active site (Fig. 5a and b).

3.4.4. Structural analysis of docking results for compound 2e

Compound 2e look like to be implicated in lot of polar interactions with residues lining pocket P2 (Fig. 5c and d). Salt bridge between conserved Cys 298 and keto oxygen of amino-pyrazole portion is also observed in case of compound 2e. S atom of carbothioamide group from compound 2e forms a bridge of hydrogen bonds connecting residues Ser 159 and Asn 160. Another series of hydrogen bonds appear to stabilize inhibitor involves N3 and N6 atoms of compound 2e that hydrogen bonds with NE2 atom from His 110, OH atom from Tyr 48 and OE1 atom of Gln 183 (Fig. 5c). Chlorobenzyl group seems to occupy P1 pocket
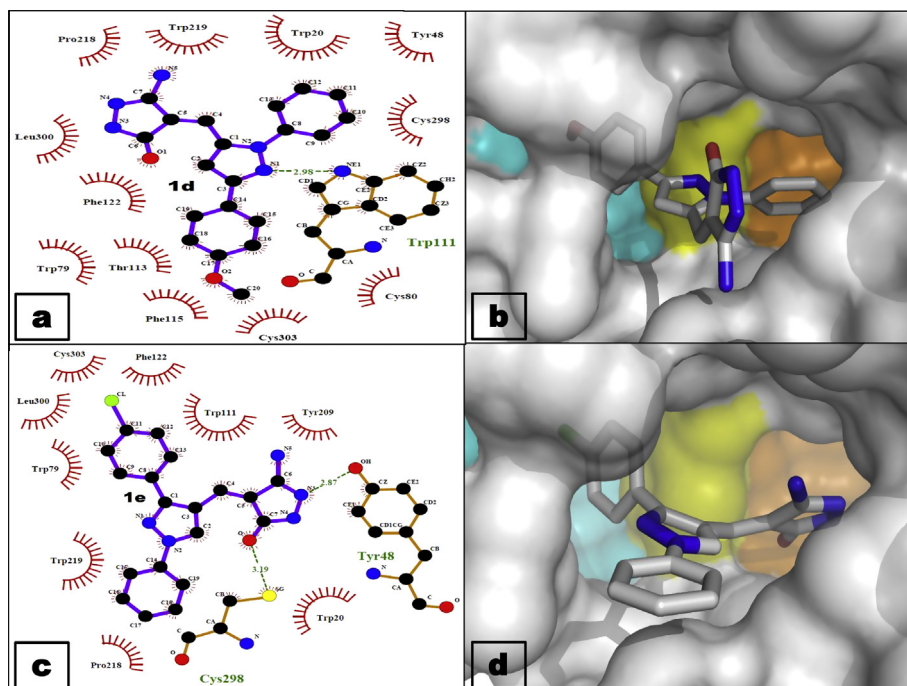
Fig. 4. Interaction of compound 1d and 1e with residues in active site of aldose reductase (a and c respectively). (b and d) represents perfect placement of two hydrophobic moieties of compound 1d and 1e in pocket P1 and P2 of aldose reductase active site.

Fig. 5. (a) Interaction of compound 2d and 2e with residues in active site of aldose reductase (a) and (c) respectively. (b) and (d) Represents perfect placement of two hydrophobic moieties of compound 2d and 2e in pocket P1 and P2 of aldose reductase active site.
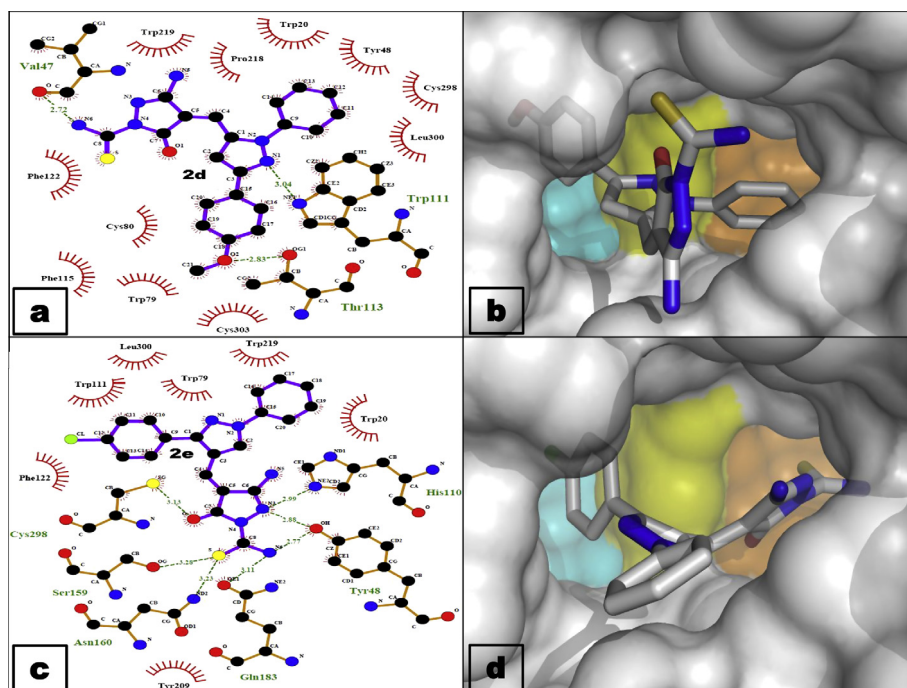
(Fig. 5d). Hydrogen bonding network as observed in this study is known to be very essential in terms of AR inhibition and has been confirmed experimentally [48,49].

4. Conclusion

Here we report synthesis of novel pyrazolone and pyrazole carbothioamide derivatives. *in vitro* testing and subsequent *in silico* analysis carried out in this study indicate that mere hydrophobicity in ligands is not sufficient for inhibition of AR. For optimal AR inhibition, excellent complementarily between active site and ligand structure is essentially required. Strategic placement of hydrophobic groups over pyrazole moiety may play a key role in achieving best inhibitory activity. Docking results on AR from this study is expected to provide springboard for initiating further detailed investigations of these compounds focusing on effective AR inhibition.

Acknowledgments

Appendix A. Supplementary material

Supplementary data associated with this article can be found, in the online version, at http://dx.doi.org/10.1016/j.bioorg.2014.02.002.

References

[1] H. King, M. Rewers, Bull. World Health Organ. 69 (1991) 643–648.
[2] R.M. Anjana, M.K. Ali, R. Pradeepa, M. Deepa, M. Datta, R. Unnikrishnan, M. Rema, V. Mohan, Indian J. Med. Res. 133 (2011) 369–380.
[3] W.H. Tang, K.A. Martin, J. Hwa, Front. Pharmacol. 3 (2012) 87–94.
[4] B.F. Johnson, R.W. Nesto, M.A. Pfeifer, W.R. Slater, A.I. Vinik, D.A. Chyun, G. Law, F.J. Wackers, L.H. Young, Diabetes Care 27 (2004) 448–454.
[5] N. Giannoukakis, Curr. Opin. Investig. Drugs 7 (2006) 916–923.
[6] M.A. Ramirez, N.L. Borja, Pharmacotherapy 28 (2008) 646–655.
[7] P.J. Oates, Curr. Opin. Investig. Drugs 11 (2010) 402–417.
[8] K.E. Schemmel, R.S. Padiyara, J.J. D'Souza, J. Diabetes Complications 24 (2010) 354–360.
[9] S.K. Srivastava, K.V. Ramana, A. Bhatnagar, Endocr. Rev. 26 (2005) 380–392.
[10] J.D. Akabari, K.B. Mehata, S.J. Pathak, H.S. Joshi, Indian J. Chem., Sect B 47 (2008) 477–480.
[11] M. Arnost, A. Pierce, E. ter Haar, D. Lauffer, J. Madden, K. Tanner, J. Green, Bioorg. Med. Chem. Lett. 20 (2010) 1661–1664.
[12] R. Venkat Ragavan, V. Vijayakumar, N. Suchetha Kumari, Eur. J. Med. Chem. 44 (2009) 3852–3857.
[13] F.A. Pasha, M. Muddassar, M.M. Neaz, S.J. Cho, J. Mol. Graph. Model. 28 (2009) 4–61.
[14] D. Castagnolo, F. Manetti, M. Radi, B. Bechi, M. Pagano, A. De Logu, R. Meleddu, M. Saddi, M. Botta, Bioorg. Med. Chem. 17 (2009) 5716–5721.
[15] A. Gursoy, S. Demirayak, G. Capan, K. Erol, E. Vural, Eur. J. Med. Chem. 44 (2009) 3852–3857.
[16] G. Mariappan, B.P. Saha, L. Sutharson, A. Haldar, Indian J. Chem., Sect B 49 (2010) 1671–1674.
[17] R. Ma, J. Zhu, J. Liu, L. Chen, X. Shen, H. Jiang, J. Li, Molecules 15 (2010) 3593–3601.
[18] P. Manojkumar, T.K. Ravi, G. Subbuchettiar, Acta. Pharm. 59 (2009) 159–170.
[19] T. Srivalli, K. Satish, R. Suthakaran, Int. J. Innov. Pharm. Res. 2 (2011) 172–174.
[20] P. Suryanarayana, P.A. Kumar, M. Saraswat, J.M. Petrash, G.B. Reddy, Mol. Vis. 10 (2004) 148–154.
[21] M.A. Miteva, F. Guyon, P. Tufféry, Nucleic Acids Res. 38 (2010) W622–W627.
[22] G.M. Morris, D.S. Goodsell, R.S. Halliday, R. Huey, W.E. Hart, R.K. Belew, A.J. Olson, J. Comput. Chem. 19 (1998) 1639–1662.
[23] R. Huey, G.M. Morris, A.J. Olson, D.S. Goodsell, J. Comput. Chem. 28 (2007) 1145–1652.
[24] A.K. Rappe, C.J. Casewit, K.S. Colwell, W.A. Goddard III, W.M. Skiff, J. Am. Chem. Soc. 114 (1992) 10024–10035.
[25] C.J. Casewit, K.S. Colwell, A.K. Rappe, J. Am. Chem. Soc. 114 (1992) 10035–10046.
[26] A.K. Rappe, K.S. Colwell, C.J. Casewit, Inorg. Chem. 32 (1993) 3438–3450.
[27] H.M. Berman, J. Westbrook, Z. Feng, G. Gilliland, T.N. Bhat, H. Weissig, I.N. Shindyalov, P.E. Bourne, Nucleic Acids Res. 28 (2000) 235–242.
[28] H. Gohlke, M. Hendlich, G. Klebe, J. Mol. Biol. 295 (2000) 337–356.
[29] R.A. Laskowski, M.B. Swindells, J. Chem. Inf. Model. 51 (2011) 2778–2786.
[30] A.C. Wallace, R.A. Laskowski, J.M. Thornton, Protein Eng. 8 (1996) 127–134.
[31] C.J. Li, B.M. Trost, Proc. Natl. Acad. Sci. USA 105 (2008) 13197–13202.
[32] R.A. Sheldon, Green Chem. 7 (2005) 267–278.
[33] N.V. Shitole, S.B. Sapkal, B.B. Shingate, M.S. Shingare, Bull. Korean Chem. Soc. 32 (2011) 35–36.
[34] N.Y. Sreedhar, M.R. Jayapal, K. Sreenivasa Prasad, P. Reddy Prasad, Res. J. Pharm. Biol. Chem. Sci. 1 (2010) 480–485.
[35] D.K. Wilson, K.M. Bohren, K.H. Gabbay, F.A. Quiocho, Science 257 (1992) 81–84.
[36] D.K. Wilson, I. Tarle, J.M. Petrash, F.A. Quiocho, Proc. Natl. Acad. Sci. USA 90 (1993) 9847–9851.
[37] H. Steuber, M. Zentgraf, C. Gerlach, C.A. Sotriffer, A. Heine, G. Klebe, J. Mol. Biol. 363 (2006) 174–187.
[38] N.A. Morjana, T.G. Flynn, J. Biol. Chem. 264 (1989) 2906–2911.
[39] V. Klimešóváa, M. Svobodaa, K. Waissera, J Kaustováb, V. Buchtac, K. Královád, Eur. J. Med. Chem. 34 (1999) 433–440.
[40] G. Cristalli, P. Franchetti, E. Nasini, S. Vittori, M. Grifantini, A. Barzi, E. Lepri, S. Ripa, Eur. J. Med. Chem. 23 (1988) 301–305.
[41] E. Lepri, G. Noeenlini, A. Barzi, G. Cristalli, P. Franchelli, Pharmacol. Res. Commun. 20 (1988) 205.
[42] P. Franchetti, E. Nasini, S. Vittori, E. Lepri, G. Nocentini, A. Barzi, in: M. Nieolini (Ed.), Platinum and Other Metal Coordination Compounds in Cancer Chemotherapy, Martinus Nijhoff Publishing, Bosion, 1987, pp. 652–656.
[43] G. Nocentini, F. Federici, P. Franchetti, A. Brazi, Cancer Res. 53 (1993) 19–26.
[44] D.H. Harrison, K.M. Bohren, D. Ringe, G.A. Petsko, K.H. Gabbay, Biochemistry 33 (1994) 2011–2020.
[45] G.K. Balendiran, M.R. Sawaya, F.P. Schwarz, G. Ponniah, R. Cuckovich, M. Verma, D. Cascio, J. Biol. Chem. 286 (2011) 6336–6344.
[46] M. Cappiello, M. Voltarelli, I. Cecconi, P.G. Vilardo, M. Dal Monte, I. Marini, A. Del Corso, D.K. Wilson, F.A. Quiocho, J.M. Petrash, U. Mura, J. Biol. Chem. 271 (1996) 33539–33544.
[47] O. El Kabbani, C. Darmanin, T.R. Schneider, I. Hazemann, F. Ruiz, M. Oka, A. Joachimiak, C. Schulze-Briese, T. Tomizaki, A. Mitschler, A. Podjarny, Proteins 55 (2004) 805–813.
[48] K.M. Bohren, C.E. Grimshaw, C.J. Lai, D.H. Harrison, D. Ringe, G.A. Petsko, K.H. Gabbay, Biochemistry 33 (1994) 2021–2032.
[49] I. Tarle, D.W. Borhani, D.K. Wilson, F.A. Quiocho, J.M. Petrash, J. Biol. Chem. 268 (1993) 25687–25693.